QUASI-CONSTANT ENVELOPE OQPSK THROUGH NONLINEAR RADIO AND AWGN CHANNEL

Qingchong Liu and Jia Li
School of Engineering and Computer Science
Oakland University
Rochester, MI

Abstract— **Quasi-constant envelope OQPSK (QCEOQPSK) signal is formed using a linear OQPSK modulator to overcome the nonlinearity caused by fully saturated RF power amplifiers. The performance of QCEOQPSK signal in AWGN channel is studied for a variety of filters in the transmitter and matched linear filters followed by hard decision in the demodulator. It is shown that at -43 dB the mainlobe of the power spectral density of the QCEOQPSK is only 77% of the bandwidth corresponding to the mainlobe of the MSK power spectrum density. At the bit error rate of 10^{-5}, the SNR degradation caused by fully saturated power amplifiers is 0.1 dB in AWGN channel compared with the ideal BER of BPSK using linear power amplifier. This is 2.3 dB better than the bit error rate of QPSK using linear power amplifier in the broadband satellite communications systems in [5]. Employing rate $1/2$ convolutional code with constraint length $K = 6$ and the Viterbi decoder, the SNR degradation is only 0.25 dB at BER=10^{-5}. Therefore, QCEOQPSK can be employed in broadband wireless or broadband satellite communication systems to achieve higher spectral efficiency, near optimal demodulation performance and significantly reduce terminal cost.**

I. INTRODUCTION

Recently many new challenges to modulation in broadband satellite and broadband wireless communications networks have emerged. These networks have to support a very large number of user terminals. To achieve high system capacity and performance, modulation methods are required to have high bandwidth efficiency and ideal bit error rate at low implementation complexity. As the data rates are much higher in broadband wireless networks, a user terminal has to transmit at high power levels than in the existing low data rate wireless communication systems [1]-[3]. To reach high transmission power and high power efficiency in mobile terminals, power amplifiers working in the fully saturated region have to be employed [4]. They cause severe nonlinear distortion to the signal. When the bandwidth is hundreds of megahertz at a carrier frequency of several dozen of gigahertz, the linear RF power amplifiers can cause significant distortion to signals [5].

This work is supported in part by the National Science Foundation under Grants ANI-0112722 and ANI-0113307.

Modulation methods are preferred to generate constant envelope in the modulated signal to tolerate the nonlinear distortion. Important early work in constant envelope modulation include the minimum shift keying (MSK) invented by Doelz and Heald in 1961 [6] and the Gaussian minimum shift keying (GMSK) by Murota and Hirade in 1981 [7]. The power spectrum density of the GMSK can be much more compact than that of the MSK signal. However, the Gaussian shaping pulse in GMSK is not a Nyquist filter and brings intersymbol interference. The intersymbol interference causes demodulation performance degradation, which is 0.46 dB in the GSM system. A maximum likelihood sequence estimator such as the Viterbi algorithm is needed in the demodulator to overcome the intersymbol interference. This increases the receiver complexity and is not suitable to broadband satellite communication systems.

Predistortion methods have been widely studied to combat nonlinearity in RF power amplifiers [8]. These methods add inverse filters in front of power amplifiers so that the combination of inverse filters and power amplifiers can have less nonlinearity. In [5] it was shown that at BER=10^{-5}, the SNR degradation caused by power amplifier distortion is 1 dB, after counting the 1.4 dB gain achieved by predistortion. Constrained by implementation complexity, these methods are unlikely to be implemented in inexpensive user terminals required by broadband wireless communications systems.

Mass production of inexpensive user terminals is also a top challenge to the broadband wireless communications industry [1]. Modulation methods are required to achieve implementation complexity as low as possible to reduce terminal cost and make mass terminal production possible [1]-[3]. The implementation complexity must be handled very carefully by both the modulator and the demodulator, considering the severe nonlinear distortion from power amplifiers.

This paper proposes the quasi-constant envelope OQPSK and studies its performance [3].

II. SYSTEM MODEL

The block diagram of a broadband wireless communication system employing fully saturated power amplifier is shown in

0-7803-7625-0/02/$17.00 ©2002 IEEE.

Fig. 1. The source data is converted from a serial stream to two parallel streams. The two parallel data streams are filtered by pulse shaping filters with the impulse response function $p(t)$. The quadrature channel data is delayed by half a symbol time to form OQPSK signal. The output of the pulse shaping filter is fed into a radio. The baseband signal at the input of the radio is

$$s_b(t) = s_I(t) + js_Q(t) \tag{1}$$

where $s_I(t) = \sum_k d_{2k}p(t - kT_s)$ is the signal to be transmitted by the in-phase channel and $s_Q(t) = \sum_k d_{2k+1}p(t - kT_s - 0.5T_s)$ is the signal to be transmitted by the quadrature phase channel. Here $\{d_i|d_i \in \{-1, +1\}\}$ is the information sequence to be transmitted and T_s is the symbol time. The radio upconverts the baseband signal to a pass-band signal centered at the carrier frequency, which is the input signal to the power amplifier and can be written as

$$s_1(t) = s_I(t)\cos(2\pi f_c t + \phi_0) - s_Q(t)\sin(2\pi f_c t + \phi_0) \tag{2}$$

where f_c is the carrier frequency and ϕ_0 is the initial carrier phase. The power amplifier in the radio amplifies the signal to the desired transmission power. The output of the radio is transmitted through the AWGN channel.

We consider a radio employing fully saturated RF power amplifier. The power amplifier completely removes the amplitude information of its input signal. The phase of the output signal is the same as the phase of the input signal. In other words, the fully saturated power amplifier does not change the phase trajectory of its input signal. Let $s_i(t)$ be the input signal to the power amplifier. The output signal $s_o(t)$ of the fully saturated power amplifier can be written as

$$s_o(t) = \begin{cases} 1 & s_i(t) > 0 \\ 0 & s_i(t) = 0 \\ -1 & s_i(t) < 0 \end{cases} \tag{3}$$

The fully saturated power amplifier is a nonlinear device which generates harmonics of the carrier and distortion to the envelope. The band-pass filter following the power amplifier removes the harmonics. Let the envelope of the input signal to the power amplifier be

$$\sqrt{s_I^2(t) + s_Q^2(t)} = \sqrt{P}(1 - y(t)) \tag{4}$$

where P is the average power and $y(t)$ is the instantaneous deviation of the signal envelope. The function $y(t)$ is a random process determined by the information sequence and the shaping pulse. The baseband equivalent signal for the transmitted signal can be written as

$$s_l(t) = \sqrt{P}(s_b(t) + n_d(t)) \tag{5}$$

where

$$n_d(t) = \frac{1 - \sqrt{s_I^2(t) + s_Q^2(t)}}{\sqrt{s_I^2(t) + s_Q^2(t)}} s_b(t) \tag{6}$$

is the distortion caused by the fully saturated power amplifier. The distortion is a random process varying with the information sequence and shaping pulse $p(t)$. The distortion expands the power density spectrum [3], makes it difficult to achieve high bandwidth efficiency, and causes degradation in demodulation performance. One can think that some shaping pulses would give nicer power density spectrum and less degradation in demodulation performance than others. However, it is less obvious to distinguish them because of the nonlinearity.

Define the signal-to-distortion power ratio at the power amplifier output as

$$\gamma\{p(t)\} \triangleq E\{\frac{\int_{-\infty}^{\infty} |s_b(t)|^2 dt}{\int_{-\infty}^{\infty} |n_d(t)|^2 dt}\} \tag{7}$$

where the ensemble average is taken in the sample space for all of the possible information sequences.

The signal-to-distortion power ratio measures the distortion to the desired siganl at the power amplifier output. When linear power amplifier is employed, $\gamma = \infty$. For constant envelope modulations such as MSK and GMSK, $\gamma = \infty$, when fully saturated power amplifier is employed. In either case, $n_d(t) = 0$.

When the envelope of the input signal to a fully saturated power amplifier has small variation, i.e., $\max|y(t)| << 1$, the distortion can be written as

$$n_d(t) = s_b(t)y(t)\sum_{n=0}^{\infty} y^n(t). \tag{8}$$

Therefore, the signal-to-distortion power ratio can be maximized by minimizing the power of $y(t)$ through choosing the appropriate shaping pulse $\{p(t)\}$.

A *quasi-constant envelope* modulation method satisfies $1 << \gamma < \infty$. We focus on quasi-constant envelope modulation methods.

The receiver is a linear receiver as shown in Fig. 1. The received signal is down-converted to baseband. The baseband signal is filtered by a filter of the impulse response function $h(t) = p(T_1 - t)$, where T_1 is the shaping pulse duration. This filter is matched to the shaping filter in the transmitter. The filter output is sampled and fed into a threshold detector.

III. Filter Design and Power Spectral Density

For the system shown in Fig. 1, we consider the square root raised cosine function, which is a smooth function and traditionally employed to achieve high bandwidth efficiency with linear RF power amplifier for AWGN channel. This function satisfies the Nyquist criterion. When it is used as both the shaping pulse in the transmitter and the matched filter in the demodulator, the matched filter output is intersymbol-interference free, if linear power amplifier is employed. Ideal demodulation performance can be achieved in this case.

Table I shows the signal-to-distortion power ratio $\gamma\{p(t)\}$ for the system in Fig. 1 employing OQPSK. The pulse shaping filter

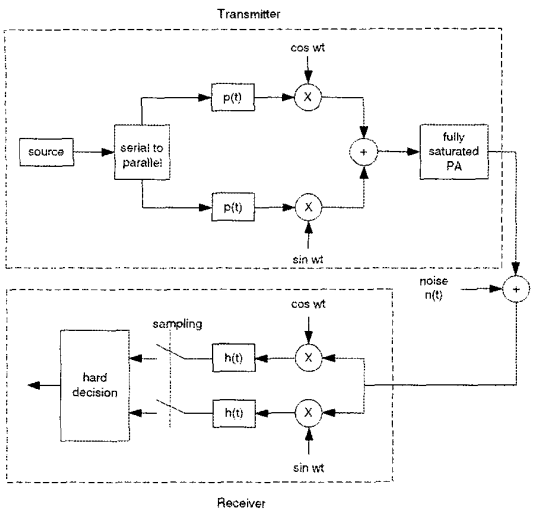

Fig. 1. Block diagram of a communication system employing fully saturated RF power amplifiers.

is of finite impulse response, which is truncated from the square root raised cosine function. The duration of the filter is L symbols and the roll-off factor is β. In other words, the pulse shaping function can be regarded as a function of β and L. It can be seen that the signal-to-distortion power ratio γ can be maximized when the roll-off factor is $\beta = 1.0$. The maximum value of the ratio γ is 21.38 dB. The effect of the shaping pulse length to the ratio γ is negligible. Therefore, the modulator output signal has quasi-constant envelope. Hereafter such a modulated signal is called the quasi-constant envelope OQPSK signal.

Fig. 2 shows the power spectral density of the quasi-constant envelope OQPSK signal amplified by a fully saturated RF power amplifier. The shaping pulse is the square-root raised cosine function with the roll-off factor $\beta = 1.0$. The power spectral densities for OQPSK with the rectangular shaping pulse and for MSK are also plotted for comparison. It can be seen that the power spectral density of the quasi-constant envelope OQPSK outperforms the power spectral densities for both OQPSK and MSK. The OQPSK signal employing the rectangular shaping pulse has constant envelope. Its shaping pulse only lasts for one symbol. The random data causes abrupt phase changes and result in high sidelobes in its power spectral density. Compared with the OQPSK signal with the rectangular shaping pulse, the quasi-constant envelope OQPSK employs a smooth shaping pulse of a longer duration. The smoothness of the square root raised cosine function and its longer than one symbol-time duration are helpful to smooth the baseband signal. Consequently the power spectral density of the quasi-constant envelope OQPSK signal has lower sidelobes than those for the OQPSK signal with the rectangular shaping pulse. The smoothed baseband signal can tolerate the nonlinearity caused by the saturated power amplifier. It can be seen that the main lobe of the power spectral density for the quasi-constant envelope OQPSK is very close to the main lobe of the power spectral density of the OQPSK signal with the rectangular shaping pulse. The same conclusions are true when we compare the quasi-constant envelope OQPSK against MSK. At -43 dB, the mainlobe of the power spectral density for the quasi-constant envelope OQPSK is only 77% of the bandwidth corresponding to the mainlobe of the MSK power spectral density. Therefore, employing the quasi-constant envelope OQPSK can save 23% of bandwidth comparing with MSK.

We conclude when fully saturated RF power amplifiers are employed, pulse shaping applied to the envelope of the baseband signal can help to smooth the baseband signal and significantly improve the spectral efficiency by reducing sidelobes in the power spectral density.

The quasi-constant envelope OQPSK can help to significantly improve bandwidth efficiency in broadband wireless and satellite communication systems. In [5] the best measured power spectral density was reported for broadband satellite communication systems, which was superior than results in [1], [2]. The system in [5] employed QPSK at 800 Mbps in the 650 MHz Ka-band channel with a linear power amplifier working at -7 dB from the saturation point. The floor of the power spectral density was -20 dB from the peak of the mainlobe. The first sidelobe occurred at about -15 dB. When the quasi-constant envelope OQPSK is employed in a system compatible to the one in [5], it can help to achieve a saving of 38.25% of the system bandwidth, or equivalently 250 MHz. Furthermore, quasi-constant envelope OQPSK allows to use fully saturated RF power amplifier and achieve dramatic cost reduction.

TABLE I

SIGNAL-TO-DISTORTION POWER RATIO γ OF OQPSK SIGNAL AMPLIFIED BY FULLY SATURATED POWER AMPLIFIER. THE SHAPING PULSE IS THE SQUARE ROOT RAISED COSINE FUNCTION WITH THE DURATION OF L SYMBOLS AND ROLL-OFF FACTOR β.

β	γ (dB)		
	$L = 8$	$L = 6$	$L = 4$
1.0	21.38	21.33	21.34
0.9	19.86	19.81	19.84
0.8	18.43	18.37	18.40
0.7	17.11	17.06	17.06
0.6	15.92	15.89	15.85
0.5	14.84	14.83	14.80
0.4	13.88	13.87	13.90
0.3	13.03	13.05	13.17

IV. DEMODULATION PERFORMANCE

As shown in Fig. 1, the receiver is a linear receiver. The in-phase signal $\Re\{r(t)\}$ is filtered by the matched filter $p(T_1 - t)$, which is the square root raised cosine filter same as the pulse

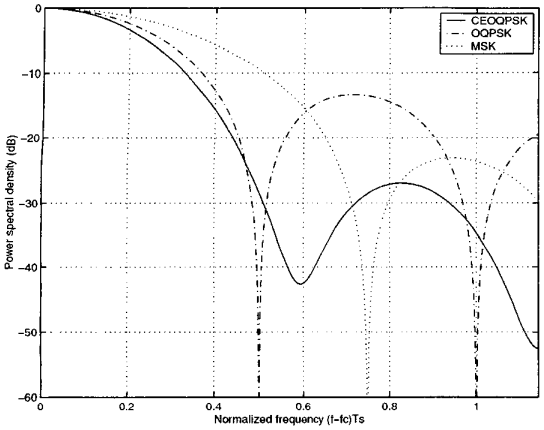

Fig. 2. Power spectral density of quasi-constant envelope OQPSK signal amplified by a fully saturated power amplifier. The horizontal axis is the normalized frequency $(f - f_c)T_s$, where T_s is the symbol time.

shaping filter in the modulator. The quadrature phase signal $\Im\{r(t)\}$ is filtered by the matched filter of the same impulse response function $p(T_1 - t)$. Both matched filters are of finite impulse response. The output of the in-phase channel matched filter is sampled at time instants $2kT_b$, where T_b is the bit time. The output of the quadrature channel matched filter is sampled at time instants $(2k + 1)T_b$. Hard decision is applied to the in-phase channel samples and the quadrature channel samples, respectively.

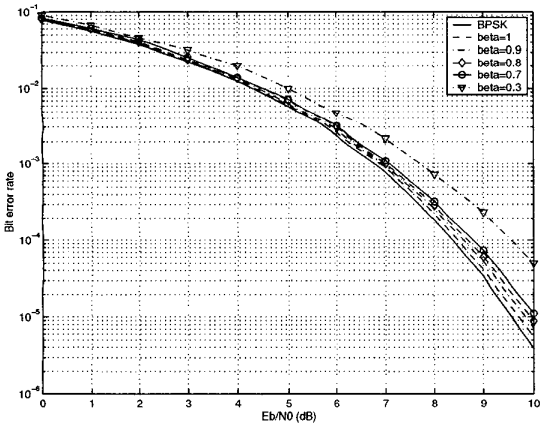

Fig. 3. Bit error rate of the quasi-constant envelope OQPSK obtained. The shaping pulse in the transmitter is the square root raised cosine function with the duration as 8 symbols. The RF power amplifier is fully saturated.

A. Coherent Demodulation

Fig. 3-5 show the simulated bit error rate for coherent demodulation. The duration of both the pulse shaping filter and the matched filter is $L = 8$ symbols, 6 symbols and 4 symbols,

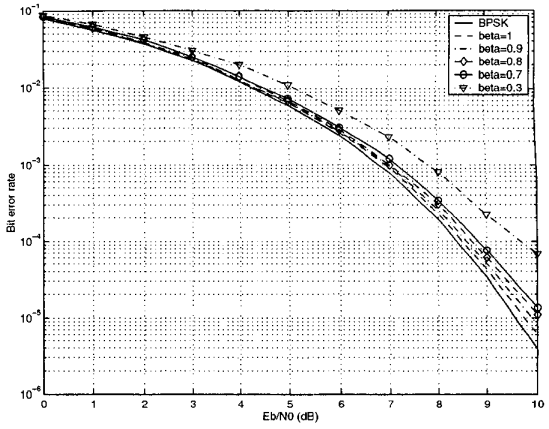

Fig. 4. Bit error rate of the quasi-constant envelope OQPSK. The shaping pulse in the transmitter is the square root raised cosine function with the duration as 6 symbols. The RF power amplifier is fully saturated.

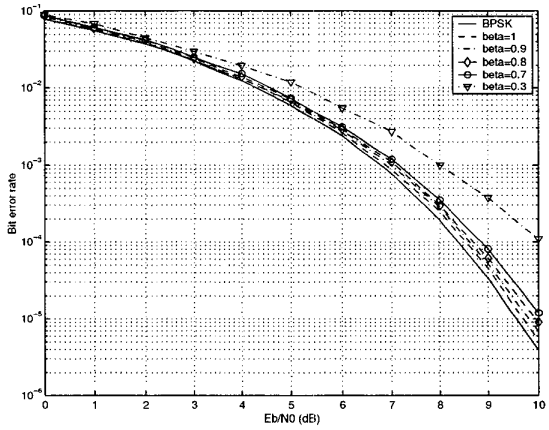

Fig. 5. Bit error rate of the quasi-constant envelope OQPSK. The shaping pulse in the transmitter is the square root raised cosine function with the duration as 4 symbols. The RF power amplifier is fully saturated.

respectively. The ideal BER for BPSK in a traditional AWGN channel is plotted as the reference. In Fig. 3, it can be seen that at BER= 10^{-5} the SNR degradation is 0.1 dB, when the duration of the filters is 8 symbols and the roll-off factor is $\beta = 1$. The degradation increases when the roll-off factor β decreases. For $\beta = 0.3$, the SNR degradation is 1.2 dB at BER=$5 \cdot 10^{-5}$.

In Fig. 4, it can be seen that the SNR degradation at BER=10^{-5} is 0.15 dB, when the duration of the filters is 6 symbols and the roll-off factor is $\beta = 1$. For $\beta = 0.3$, the SNR degradation is 1.3 dB at BER=10^{-4}.

In Fig. 5, it can be seen that the SNR degradation at BER=10^{-5} is also 0.15 dB, when the duration of the filters is 4 symbols and the roll-off factor $\beta = 1$. For $\beta = 0.3$, the SNR degradation is 1.6 dB at BER=10^{-4}.

We can conclude that when linear receiver and hard decision are employed, the quasi-constant envelope OQPSK can achieve

near optimum demodulation performance compared with BPSK, when the square root raised cosine function is employed as the pulse shaping filter and the matched filter with the roll-off factor $\beta = 1$ and the duration is not less than 4 symbols. For $0.7 \leq \beta \leq 1$, increasing the shaping pulse duration to more than 4 symbols can not bring apparent improvement to BER performance. This is because the fluctuation in the modulated signal envelope is small and the extended shaping pulse makes negligible difference to smooth the signal. For $\beta = 0.3$, increasing the shaping pulse duration can improve BER performance. When β is small, the fluctuation in the modulated signal envelope is large and the extended shaping pulse can contribute to smooth the signal. For practice, we recommend $\beta \in [0.7, 1]$ and the shaping pulse duration to be 6 symbols.

B. Timing Error Effect

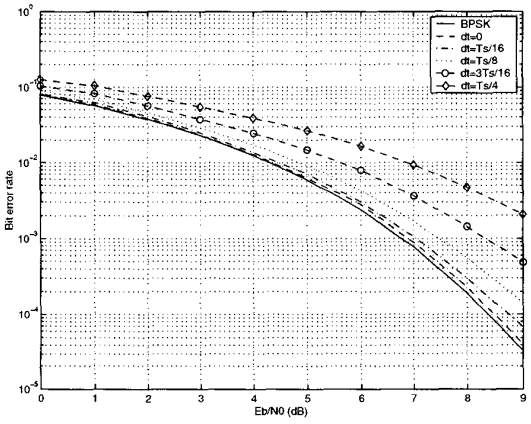

Fig. 6. Bit error rate of the quasi-constant envelope OQPSK for different timing errors. The RF power amplifier is fully saturated.

Simulation has shown that the bit error rate is an even function of the timing error, same as in a linear channel. Fig. 6 shows the simulated BER versus SNR for different timing error. It can be seen that the timing error dt can cause large degradation in SNR, when $|dt| > T_s/16$. Therefore, symbol timing estimator with the standard deviation not larger than $T_s/16$ is needed.

In [9], it is shown that the Cramer-Rao bound for the maximum likelihood symbol timing estimation is

$$(\frac{\sigma_\tau}{T_b})^2 = \frac{1}{2T_\tau(P/N_0)(T_bD)^2} \tag{9}$$

where $T_\tau = NT_s$, N is the number of symbols used for timing estimation, P is the average power, $N_0/2$ is the power of the AWGN and

$$(T_bD)^2 = \frac{\pi^2}{12} + (\frac{\pi^2}{4} - 2)\beta^2. \tag{10}$$

Therefore, the number of symbols needed for symbol estimation such that $\sigma_\tau \leq T_s/16$ is

$$N \geq \frac{16}{\frac{E_b}{N_0}[\frac{\pi^2}{12} + (\frac{\pi^2}{4} - 2)\beta^2]}. \tag{11}$$

C. Phase Error Effect

Phase error can be caused by either phase estimator or phase-locked loop for carrier recovery in the demodulator. Fig. 7 plots the BER versus the SNR for different phase errors. It can be seen that the BER is sensitive to phase errors. When the phase error is $\pi/64$, the SNR degradation is 0.2 dB at BER $= 10^{-4}$. Usually phase estimator is employed in the receiver for initial phase estimation. It is recommended that the standard deviation of the phase estimator to be less than $\pi/64$.

In [9], it is shown that the Cramer-Rao bound for the unbiased maximum-likelihood phase estimator is

$$\sigma_\phi^2 \geq (4NE_b/N_0)^{-1} \tag{12}$$

where N is the number of symbols employed for phase estimation.

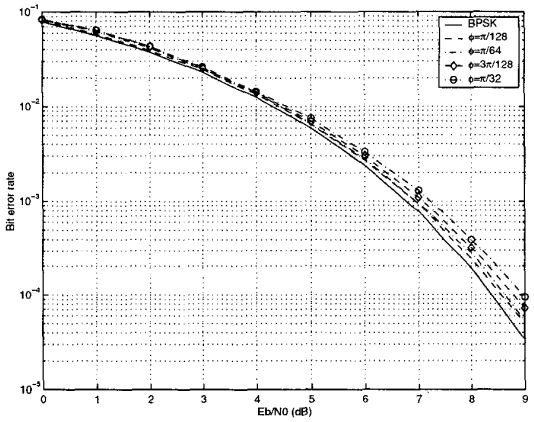

Fig. 7. Bit error rate for different phase errors.

In broadband wireless and satellite communications, usually a preamble is employed for packet detection and parameter estimation. The length of symbols required for phase and timing estimation can be chosen according to (11) and (12). Results shown in Fig. 7 is needed for phase-locked loop design in carrier recovery, which can be designed properly by following [10], [11].

V. Coded Performance

The rate $1/2$ convolutional code with the constraint length $K = 6$ is applied to communication systems employing the quasi-constant envelope OQPSK and fully saturated RF power amplifiers. The decoder is the Viterbi decoder using soft decision. Fig. 8 shows the simulated bit error rate in AWGN channel. The bit error rate of a compatible system employing the

ideal linear RF power amplifier is also simulated for comparison. The simulated bit error rate for the system employing the ideal linear RF power amplifier in AWGN channel matches well with the coded performance for BPSK in [11]. It can be seen that the fully saturated RF power amplifier causes small SNR degradation. When the bit error rate is 10^{-5}, the degradation is only 0.25 dB. Therefore, the SNR degradation caused by the fully saturated RF power amplifier is tolerable in a practical system.

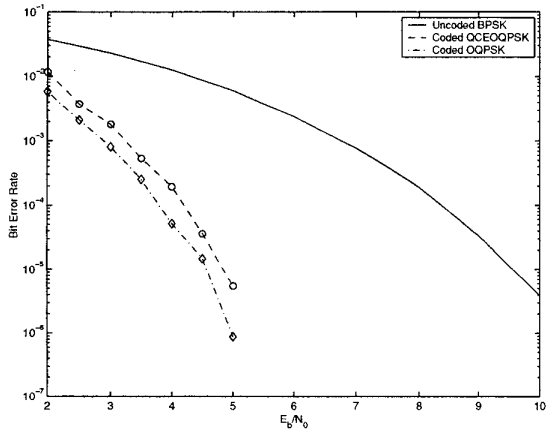

Fig. 8. Bit error rate of a communication system in AWGN channel. The solid line is the bit error rate for BPSK. The dash line is for the system employing OQPSK, linear RF power amplifier, rate $1/2$ convolutional code with $K = 6$ and Viterbi decoder. The dash-dot line is for the system employing the quasi-constant envelope OQPSK, fully saturated RF power amplifiers, rate $1/2$ convolutional code with $K = 6$ and Viterbi decoder.

VI. Conclusions

Quasi-constant envelope OQPSK is proposed to achieve near optimal bit error performance, high bandwidth efficiency, and significant terminal cost reduction for broadband wireless and satellite communications systems employing fully saturated RF power amplifiers. It is shown that applying the square root raised cosine function with the roll-off factor $\beta = 1$, the signal-to-distortion power ratio of the fully saturated power amplifier can reach 21.38 dB. At -43 dB, the mainlobe of the power spectral density for the quasi-constant envelope OQPSK is only 77% of the bandwidth corresponding to the mainlobe of the MSK power spectral density. The receiver is a linear receiver employing two linear filters matched to the pulse shaping filters in the transmitter. Hard decision is employed directly to the matched filter output signals. When transmitted by fully saturated radio in AWGN channel, the quasi-constant envelope OQPSK can achieve near optimal bit error rate performance compared with BPSK using linear power amplifiers. At BER=10^{-5}, the SNR degradation is 0.1 dB when the duration of the filter is 8 symbols and $\beta = 1$. The degradation is increased when β decreases. Reducing the filter duration to 4 symbols causes negligible SNR degradation when $0.7 \leq \beta \leq 1$. Effects of the timing error and the phase error to demodulation performance is investigated. Requirements to timing estimation and phase estimation are provided. When rate $1/2$ convolutional code with the constraint length $K = 6$ is applied the communication system employing quasi-constant envelope OQPSK and fully saturated power amplifier, the SNR degradation is 0.25 dB at the bit error rate of 10^{-5}. Therefore, the quasi-constant envelope OQPSK can help to achieve near optimal performance in broadband wireless and satellite communications systems using fully saturated power amplifiers.

References

[1] E. M. Wildauer, M. J. Pender, Jr., and J. E. Ohlson, "Modulation method and system using constant envelope ODSCDMA with low out-of-band emissions for non-linear amplification," US Patent No. 5,903,555, May 11, 1999 (filed Oct. 30, 1996).

[2] C. A. Herbst, L. J. Fruit, J. A. Wilkerson, Jr., "Constant envelope continuous phase frequency shift key modulation apparatus and method at radio frequency," US Patent No. 5,812,604, Sept. 22, 1998 (filed July 16, 1996).

[3] Q. Liu, "Performance evaluation of OQPSK and $\frac{\pi}{4}$ QPSK and MSK passing through a slicer," *Hughes Network Systems Techn. Report*, December 14, 1996.

[4] M. D. Weiss, F. H. Raab, and Z. Popovic, "Linearity of X-band class-F power amplifiers in high-efficiency transmitters," *IEEE Trans. Microwave Theory Tech.*, vol. 49, pp. 1174-1179, June 2001.

[5] S. Vaughn and R. Sorace, "Demonstration of the TDRS Ka-band transponder," *Proc. 2000 IEEE Military Commun. Conf.*, vol. 2, pp. 1055-1065, 22-25 Oct., 2000, Los Angeles, CA.

[6] M. I. Doelz and E. H. Heald, "Minimum shift data communication system," US Patent No. 2,977,417, March 1961.

[7] K. Murota and K. Hirade, "GMSK modulation for digital mobile radio telephony," *IEEE Trans. Commun.*, vol. 29, pp. 1044-1050, July 1981.

[8] A. N. D'Andrea, V. Lottici, and R. Reggiannini, "RF power amplifier linearization through amplitude and phase predistortion," *IEEE Trans. Commun.*, vol. 44, pp. 1477-1484, Nov. 1996.

[9] T. Alberty, "Frequency domain interpretation of the Cramer-Rao bound for carrier and clock synchronization," *IEEE Trans. Commun.*, vol. 43, pp. 1185-1191, Feb./March/Apr. 1995.

[10] A. J. Viterbi, *Principles of Coherent Communication*, New York: McGraw-Hill, 1966.

[11] J. A. Heller and I. M. Jacobs, "Viterbi decoding for satellite and space communication," *IEEE Trans. Commun.*, vol. 19, pp. 835-848, Oct. 1971.